

Article

Fabrication and Optimization of a Lipase Immobilized Enzymatic Membrane Bioreactor based on Polysulfone Gradient-Pore Hollow Fiber Membrane

Peng-Cheng Chen ¹, Zhen Ma ², Xue-Yan Zhu ³, Da-Jing Chen ² and Xiao-Jun Huang ^{3,*} 

¹ The Key Laboratory of Industrial Biotechnology, Ministry of Education, School of Biotechnology, Jiangnan University, Wuxi 214122, China; chenpengcheng@jiangnan.edu.cn

² School of medicine, Hangzhou Normal University, Hangzhou 311121, China; mazhen-mz@foxmail.com (Z.M.); djchen@hznu.edu.cn (D.-J.C.)

³ MOE Key Laboratory of Macromolecular Synthesis and Functionalization, Department of Polymer Science and Engineering, Zhejiang University, Hangzhou 310027, China; 21429008@zju.edu.cn

* Correspondence: hxjzxh@zju.edu.cn; Tel.: +86-571-8827-6294

Received: 4 April 2019; Accepted: 16 May 2019; Published: 28 May 2019



Abstract: Enzymatic membrane bioreactors (EMBRs) possess the characteristic of combining catalysis with separation, and therefore have promising application potentials. In order to achieve a high-performance EMBR, membrane property, as well as operating parameters, should give special cause for concerns. In this work, an EMBR based on hollow fiber polysulfone microfiltration membranes with radial gradient pore structure was fabricated and enzyme immobilization was achieved through pressure-driven filtration. Lipase from *Candida rugosa* was used for immobilization and EMBR performance was studied with the enzymatic hydrolysis of glycerol triacetate as a model reaction. The influences of membrane pore diameter, substrate feed direction as well as operational parameters of operation pressure, substrate concentration, and temperature on the EMBR activity were investigated with the production of hydrolysates kinetically fitted. The complete EMBR system showed the highest activity of $1.07 \times 10^4 \text{ U} \cdot \text{g}^{-1}$. The results in this work indicate future efforts for improvement in EMBR.

Keywords: enzymatic membrane bioreactor; gradient-pore membrane; lipase; filtration; hydrolysis

1. Introduction

Enzymatic membrane bioreactors (EMBRs), endowed with synergistic catalysis and separation functions, can create a favorable thermodynamic and kinetic process. In recent years, EMBRs have grasped much attention in fields of food and medical industry, chemical manufacturing, and environmental protection [1–6]. Generally, EMBRs have the characteristics of elongating the lifetime of enzymes and improving their reusability, and the porous structure of membranes allows for a high specific surface area and relatively low diffusion resistance. Nevertheless, up to now, the usage of immobilized enzymes in industrial biocatalytic processes is still limited, and problems such as fabricating efficient enzyme-immobilized membranes and constructing controllable enzyme catalysis and separation systems remain to be solved in the research and practical application of EMBRs [7–9].

In EMBRs, membranes act as the support for enzymes, which directly influence enzyme loading and activity of the immobilized enzyme; also, the pore microstructure is connected with the stability and filtration performance of the membranes [10–12]. As a result, membranes should be carefully selected. Polysulfone (PSF) hollow fiber membrane is often used for developing EMBRs because of

its chemical resistance, thermal stability, and ease in module manufacturing and operation [13–15]. According to the mass transfer behavior of microporous membranes, increasing pore size helps to increase membrane permeability; whereas, in practical application, excessively large pore structures could impair the overall mechanical properties of the membranes [16,17]. On the other hand, decreasing pore size helps to increase the specific area for enzyme immobilization, and a higher enzyme loading helps to promote the catalytic efficiency of EMBRs, whereas the problem of enzyme blocking and membrane fouling accompanied [18–20]. Therefore, membranes with high porosity to enable good permeability and a high specific area for enzyme attachment, meanwhile with heterogeneous pores to ensure good mechanical stability and anti-fouling property are desirable.

PSF microfiltration membranes with radial gradient pore structure (RGM-PSF membranes), the pore size of which reduces gradually from the inner side to the outer side, have been selected as supports in this work. This pore structure is considered to provide increased sites for enzyme immobilization and allow for the fixation of enzyme molecules in the three-dimensional network structure of the membrane, which helps to give improved performance including high flux, low osmosis resistance, and outstanding catalytic efficiency [21]. Generally, enzyme immobilization onto membranes can be achieved by physical adsorption, entrapment, and covalent attachment [22]. Since PSF membranes comprise a small number of end functional groups, many surface modification methods have been developed to increase the number of functional groups on the membranes to improve enzyme loading by covalent attachment [23–26]. Compared to the chemical immobilization method, physical adsorption is gentler, and through simple pressure-driven filtration, enzyme molecules can be immobilized in the pores of RGM-PSF by hydrophobic interactions.

Generally, the immobilization process can protect enzymes from shear damages and enzyme leakage, whereas it also introduces mass transfer limitation [27]. Protein-substrate interaction is another important aspect influencing bioreactor efficiency since more products can be produced if the substrates have good full contact with the enzyme. Operational parameters such as operating pressure, substrate concentration, and temperature also influence the performance of an EMBR undoubtedly. Up to now, evaluating the performance of an EMBR is still a complicated task given the many variables involved in affecting enzyme activity, stability, and reusability, and they differ widely from authors to authors, which makes a comparison between different EMBRs difficult. In this regard, the catalytic reaction rate determined by mathematic fitting may be a helpful indicator in evaluating EMBR efficiency apart from bioreactor activity, since it rules out the difference in the definition of bioreactor activity. Moreover, for one established EMBR, studying its operation efficiency systematically requires substantial effort and a large number of enzymes and reagents. Taken this aspect into consideration, a scaled down bioreactor apparatus is suitable for the fundamental research of the practicability of an EMBR.

In this study, a lab-scale EMBR was fabricated based on the RGM-PSF membranes. Lipase from *Candida rugosa* (CRL) was retained in the membrane by pressure-driven filtration. The changes in pore size and structure of RGM-PSF membranes after immobilization were characterized. An investigation of EMBR performance on glycerol triacetate (TA) hydrolysis as the model reaction was conducted, with special emphasis on membrane pore diameter in order to evaluate the effects of the mass transfer resistance and enzyme-substrate interaction. In addition, the influences of substrate feed direction and operational parameters on the EMBR activity were studied. This trial is expected to exhibit the advantages and application of microfiltration membranes with a specific pore structure.

2. Results and Discussion

2.1. CRL Immobilization in RGM-PSF Membranes Based EMBR

RGM-PSF membranes with four different pore sizes were used in this work with morphology characterization presented in Table S1. Large pores distributed on the inner surface of the membranes, and smaller ones distributed radially to the outer surface. The thickness of these membranes was similar. Pores diameters were 0.34, 0.54, 0.78, and 1.14 μm , respectively, from membrane #1 to membrane #4.

Figure 1 depicted the curves of enzyme loading and trans-membrane pressure during the enzyme immobilization period. According to this figure, lipase went through a fast immobilization process in these EMBRs and could reach an adsorption balance within 150 min. Enzyme loading was within the range of 27.4 ± 1.7 mg/g to 28.2 ± 1.9 mg/g for these four pore sizes, indicating the pore diameter had little influence on enzyme loading. Moreover, the enzyme loading was noted to be comparable to that obtained from nanofiber membranes and was much higher than that obtained from the traditional PSF hollow fiber [28,29]. This phenomenon showed that the special porous character of the RGM-PSF membranes could greatly improve the specific area and thus favored enzyme immobilization. Trans-membrane pressure increased with time until reaching equilibrium during the immobilization process, and this equilibrium value increased with the decrease of pore diameter for these four membranes.

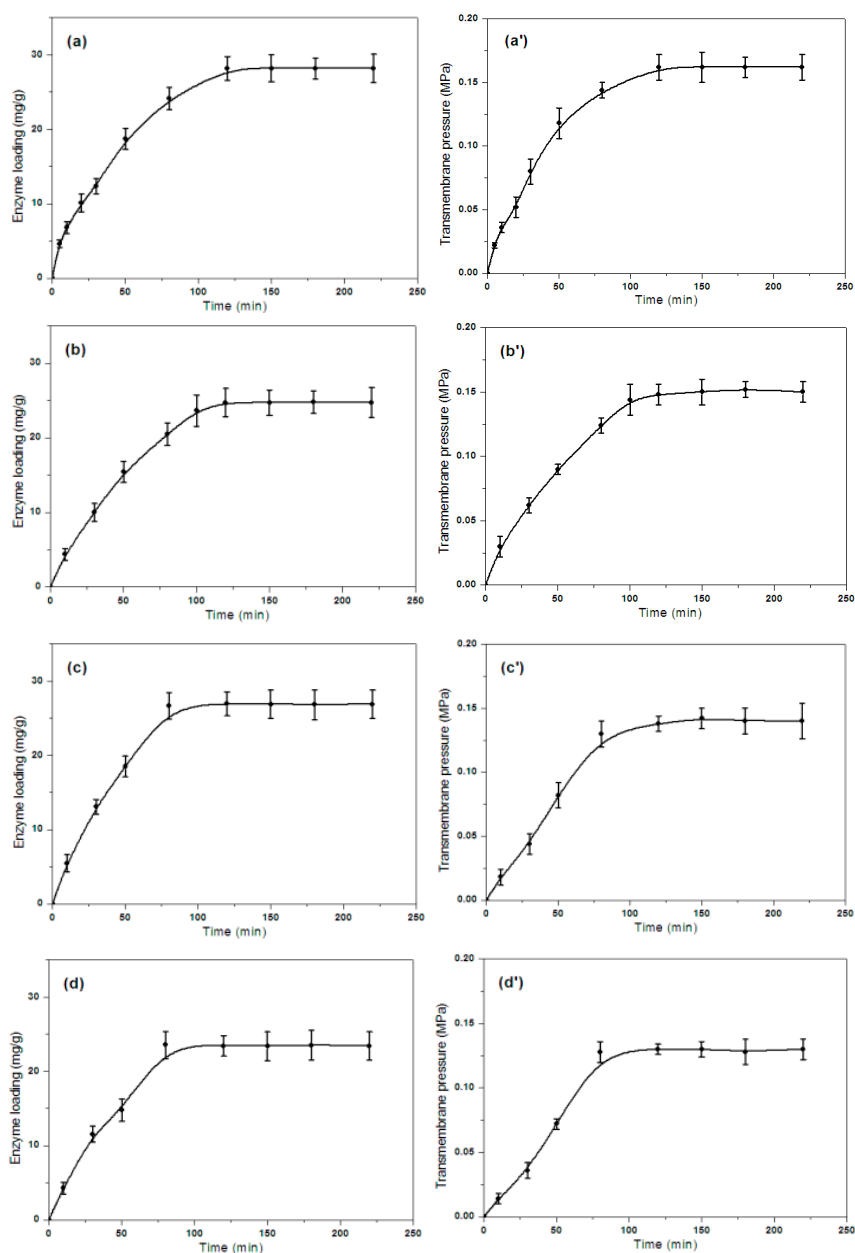


Figure 1. Effect of time on enzyme loading and trans-membrane pressure for polysulfone microfiltration membranes with radial gradient pore structure (RGM-PSF membranes) with different pore sizes. (a,a'): membrane #1; (b,b'): membrane #2; (c,c'): membrane #3; (d,d'): membrane #4.

After the CRL immobilization process, the pore size of membranes decreased, but no obvious change in membrane morphology was observed (Table S2). According to the particle size distribution of CRL dissolved in phosphate buffer solution (PBS 0.05 M, pH 7.0) (Figure S1), the average diameter of free CRL was 68.8 nm. This value was bigger than the diameter of a single CRL molecule, which indicated that a few CRL molecules combined in aqueous solution. Moreover, this value was much smaller than the pore diameters of pristine membranes; thus, lipase could enter the membrane pores easily through filtration.

Figure 2 presented the decrease in pore diameter and water flux after CRL immobilization. According to this figure, there was about a 50% decrease in pore diameter for each membrane. It was noted that the size of pore reduction was larger than that of free CRL in solution, indicating an inevitable aggregation of lipase in the pore. Moreover, the tendency of lipase aggregation increased with the increase of pristine membrane pore size, which may influence EMBR performance. The adsorbed lipase in the membrane pores changed the pore size, porosity, and pore surface properties of the membranes as well, resulting in a decreased permeability of the lipase-loaded membrane.

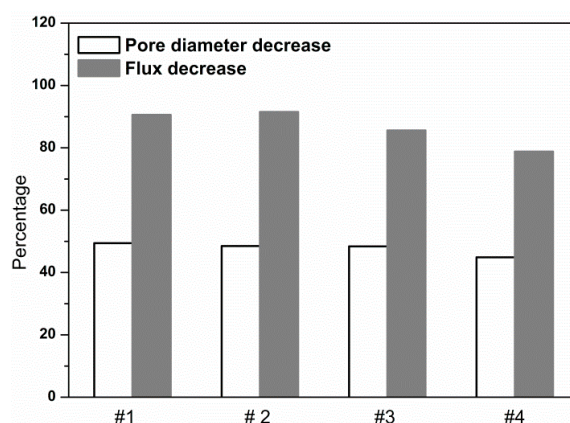


Figure 2. Pore diameter and flux decrease of the membranes after *Candida rugosa* (CRL) immobilization.

2.2. Effect of Pore Diameter on the Efficiency of EMBR

In this part of the research, a 0.2 M TA aqueous solution was used to evaluate the effect of pore diameter on the efficiency of EMBR. Acetic acid production in EMBRs was shown in Figure 3. During the operation period, the temperature was fixed at 25 °C, and the feed direction of the substrate was from the inner surface to the outer surface of the membrane (I/O). A blank experiment was conducted with the same apparatus but without the lipase immobilization process, and no acetic acid was produced throughout the operation period. In Figure 3, the amount of acetic acid increased with time during the operational period, indicating the enzymatically hydrolytic reaction was in progress. The production of acetic acid with time showed a linear trend and was regressed using the linear function to determine the volumetric reaction rate (V_r , $\text{mmol}\cdot\text{L}^{-1}\cdot\text{min}^{-1}$) of this hydrolytic reaction. Solid lines in the figure gave the regression results. V_r was calculated from the slope and was summarized in Table S3. Figure 3a showed the production of acetic acid under the operating pressure of 0.17 MPa. V_r increased with the decrease in membrane pore diameter, and from membrane #4 to membrane #1, the bioreactor activity increased from 3.14×10^3 to $5.86 \times 10^3 \text{ U}\cdot\text{g}^{-1}$. At a definite operation pressure, the decrease in membrane pore diameter led to an increase in mass transfer resistance for the fluid inside the membrane, and the velocity of the fluid inside membrane decreased. In this situation, the hydrolysis product may not flow out of the membrane in time, and thus cannot be titrated timely by NaOH solution and led to a decrease in V_r . Nevertheless, the decrease in fluid velocity may offer more chances for protein-substrate interactions, which helped to improve the bioreactor activity. According to the results shown in Figure 3a and Table S3, the unfavorable effect brought by the increased mass transfer resistance cannot compete to the favorable effect brought by the fuller contact of the substrate with the immobilized CRL, and thus the highest activity was obtained in the EMBR equipped with membrane #1.

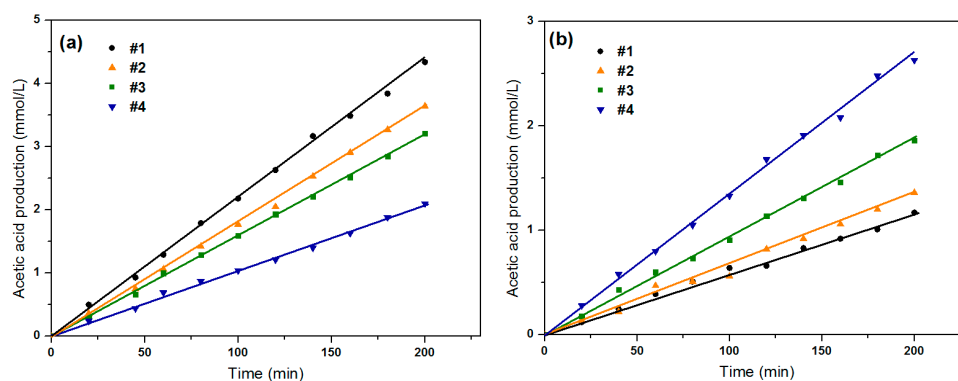


Figure 3. Acetic acid production versus time as affected by different pore diameters (pressure: (a) 0.17 MPa, (b) 0.07 MPa; temperature: 25 °C; substrate: 0.20 M TA solution).

To verify the discussion above, EMBRs were operated under a lower pressure of 0.07 MPa, with other operational conditions remained the same. The acetic acid production versus time was shown in Figure 3b. The result was opposite to that shown in Figure 3a, and the highest bioreactor activity of $3.64 \times 10^3 \text{ U}\cdot\text{g}^{-1}$ was achieved in EMBR equipped with membrane #4. This result demonstrated that under this pressure, the increased mass transfer resistance played a key role in determining the bioreactor activity.

Based on this study, pore diameter influenced the bioreactor activity by means of affecting the mass transfer resistance of the fluid in the membrane and the contact of the substrate with immobilized lipase.

2.3. Effect of Substrate Feed Direction on the Efficiency of EMBR

In this part of the study, EMBR equipped with membrane #1 was used, and the operating pressure and temperature were fixed at 0.17 MPa and 25 °C. Results were presented in Figure 4 and Table S3. A higher bioreactor activity was obtained under a substrate feed direction of I/O, which may be ascribed to two reasons. First, since the substrate feed direction of CRL solution was I/O in the enzyme immobilization process, a number of lipases were immobilized on the inner surface of the membrane; when the substrate feed direction was from the outer surface to the inner surface of the membrane (O/I), the accessibility of substrate to the lipases immobilized on the inner surface of the membrane was lowered. Second, when the substrate feed direction was O/I, the pore size increased gradually with this direction, which led to a higher membrane flux than that when the substrate feed direction was I/O (the pure water flux was $2.2 \times 10^3 \text{ L}\cdot\text{m}^{-2}\cdot\text{h}^{-1}\cdot\text{MPa}^{-1}$ when the feed direction was I/O, whereas that for O/I was $3.6 \times 10^3 \text{ L}\cdot\text{m}^{-2}\cdot\text{h}^{-1}\cdot\text{MPa}^{-1}$); under this circumstance, the fluid velocity increased, which lowered the accessibility of the immobilized lipases to the substrates.

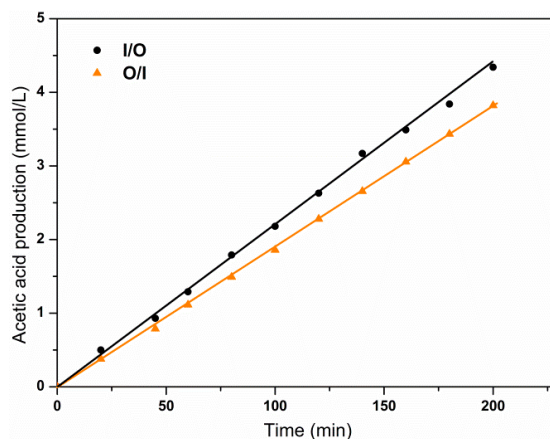


Figure 4. Acetic acid production versus time as affected by substrate feed direction of O/I and I/O (pressure: 0.17 MPa, temperature: 25 °C, substrate: 0.20 M TA solution).

2.4. Effect of Operational Parameters on the Efficiency of EMBR

In the study of operational parameters on the efficiency of EMBR, bioreactors equipped with membrane #1 were used with a substrate feed direction of I/O. Different parameters of operation pressure, substrate concentration, and temperature were considered, with the linear fitting results and bioreactor activity summarized in Table S3.

2.4.1. Effect of Operation Pressure on the Efficiency of EMBR

When the concentration of TA and temperature are 0.20 M and 25 °C, the acetic acid production under the operation pressures of 0.07, 0.10, 0.14, and 0.17 MPa is depicted in Figure 5a. The activities of EMBR increased with the increase in operation pressures. A higher operation pressure brought about an increased EMBR activity. When the operation pressure was 0.17 MPa, the bioreactor activity was $5.86 \times 10^3 \text{ U}\cdot\text{g}^{-1}$; this value was 2.31 times higher than that when the operation pressure was 0.07 MPa. On the one hand, a higher operation pressure helped the substrate penetrate into the membrane pore, and thus increased the accessibility of the substrates to the immobilized lipases. On the other hand, a higher operation pressure can decrease the boundary layer on the aqueous side of the membrane to deduce the mass transfer resistance; and in this circumstance, the mass transfer rate of the acetic acid from the reaction microenvironment to the aqueous phase bulk was increased, thus acetic acid could be titrated by NaOH solution in time to promote the hydrolysis reaction [30].

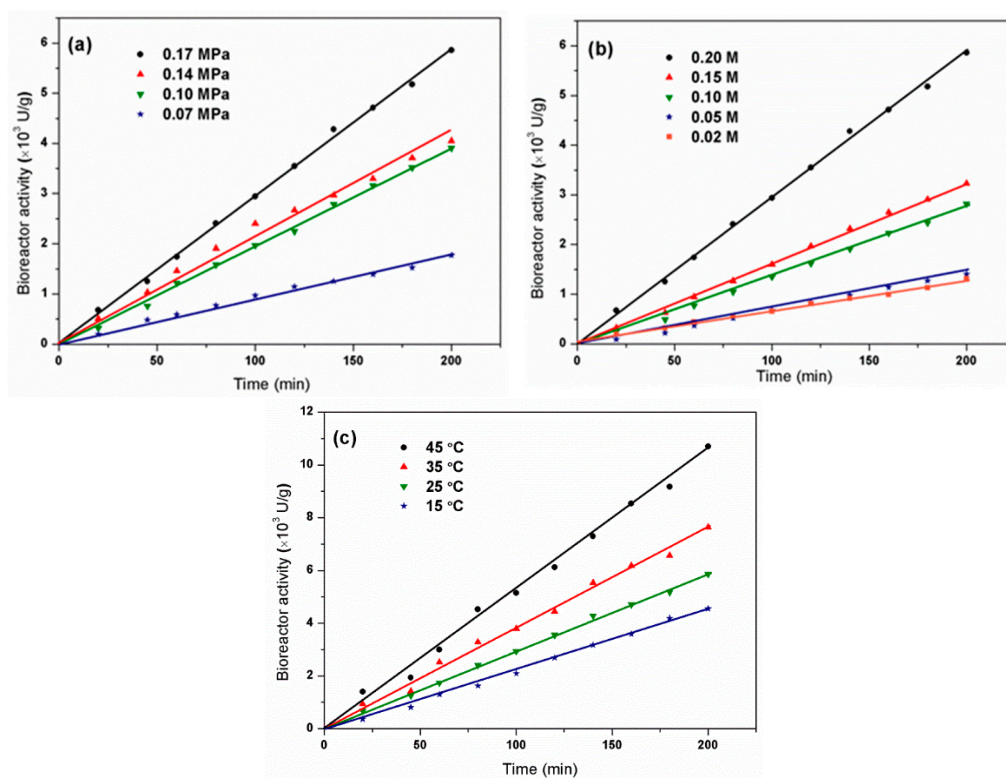


Figure 5. Acetic acid production versus time as affected by (a) operation pressure, (b) substrate concentration, and (c) temperature.

2.4.2. Effect of Substrate Concentration on the Efficiency of EMBR

Figure 5b showed the effect of substrate concentration on the efficiency of EMBR under the operation pressure and temperature of 0.17 MPa and 25 °C. It is encouraging to see the production of acid in this work was comparable to that obtained in the enzyme-immobilized membrane bioreactor, which was constructed with nano-scale fiber membranes [31]. A higher substrate concentration helped to improve the bioreactor activity and a maximum activity of $5.86 \times 10^3 \text{ U}\cdot\text{g}^{-1}$ was obtained at a 0.20 M

of substrate concentration. This was because the increase in substrate concentration enhanced the accessibility of the substrates to the immobilized lipases and thus improved the occurrence of the hydrolysis reaction. Moreover, V_{\max} and K_m were respectively assayed for the free and immobilized lipases. V_{\max} reflects the intrinsic characteristics of the immobilized enzyme but may be affected by diffusion constraints. K_m reflects the effective characteristics of the enzyme and depends upon both partition and diffusion effects. In this work, the value of K_m was 45.6 ± 2.57 mM for the free lipase, while that was 88.6 ± 4.43 mM for the immobilized lipase; the V_{\max} value of 3.56 ± 0.03 mol·min⁻¹ for the free lipase was found to be higher than that for the immobilized one (2.08 ± 0.02 mol·min⁻¹). This was either due to the conformational changes of the enzyme resulting in a lower possibility of forming a substrate-enzyme complex, or less accessibility of the substrate to the active sites of the immobilized enzyme caused by the increased diffusion limitation.

2.4.3. Effect of Temperature on the Efficiency of EMBR

Figure 5c shows the acetic acid production under different temperatures. In this study, the operation pressure was 0.17 MPa with a 0.20 M of TA concentration. Bioreactor activity was observed to increase when the temperature increased from 15 to 45 °C. Compared with the bioreactor activity of 4.55×10^3 U·g⁻¹ at 15 °C, there was a more than two times enhancement to 1.07×10^4 U·g⁻¹ at 45 °C. The optimal temperature of CRL at 45 °C found on the Sigma homepage may explain the result. Also, the higher bioreactor activity at a higher temperature may be explained by the fact that the interaction between the lipase and the membrane reduced the flexibility of the lipase conformations and thus an increased temperature was required for the rearrangement of the lipase molecule to assume a catalytically active conformation. Another possible explanation is that the mass transfer resistances for the substrate and hydrolysis product were diminished at a higher temperature, which can improve the bioreactor activity.

2.5. Reusability of Immobilized Enzymes

The ability to reuse the immobilized lipase is of vital importance for guaranteeing the practicability of repeated batch or continuous reaction in EMBRs. In the reusability studies, EMBR equipped with membrane #1 was used. The substrate feed direction was I/O, with the operation pressure, substrate concentration and temperature fixed at 0.17 MPa, 0.20 M and 45 °C, respectively. Bioreactor activity in the first batch was set as 100%, and the activities in the subsequent batches were compared to it. Results were presented in Figure 6. Altogether nine batches were operated. An obvious decrease in bioreactor activity appeared in the first three batches, and 31.6% of the original activity was lost after the third batch. Then a relatively stable state was observed from the fourth to seventh batch, and the bioreactor activity retention was 54.4% after the seventh batch. After nine cycles of batch operation, 38.6% of the original bioreactor activity remained. The rapid activity decrease in the first three batches might be ascribed to the leach of physically attached lipases. Moreover, the activity loss was inevitable, considering the lipases inactivation by continuous use.

According to the reusability results, although physical immobilization through filtration is simple, immobilized lipases are not stable in practical repeated usage due to the relatively weak interactions. In this context, chemical binding of lipases can be adopted in the future to enhance the membrane-enzyme interaction. Ulbricht emphasized that maintaining membrane characteristics should be the priority in order to prevent serious reduction on membrane performance (i.e., flux and selectivity) [32]. In this regard, functional groups such as carboxyl, hydroxyl and amine groups can be introduced onto the surface of polysulfone membranes through different surface modification methods without affecting the bulk properties and to covalently interact with lipases [8]. Ranieri et al. prepared asymmetric ceramic hollow fiber membranes for covalent immobilization of lipase, and the lipase-immobilized membrane can be repeatedly used for six times without obvious activity loss. Moreover, crosslinking lipases into aggregates to increase the size of lipase particles can also be

considered to reduce enzyme leaching and improve the application stability of the EMBR [33], but with the size of lipase aggregates tailored in order not to sacrifice protein-substrate interactions.

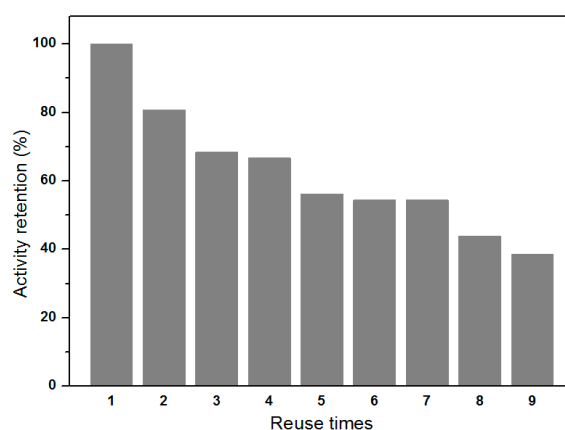


Figure 6. Reusability of the CRL-immobilized hollow fiber membranes in the bioreactor.

3. Materials and Methods

3.1. Materials

CRL powder (1150 units per mg solid), bovine serum albumin (BSA, molecular mass: 67 kDa), Bradford reagent, and TA were obtained from Sigma Aldrich Chemical Co. (St. Louis, MO, USA) and used without further purification. Fluorescein isothiocyanate-labeled CRL (FITC-CRL) was purchased from Beijing Protein Innovation Co., Ltd. (Beijing, China). All the other chemicals were of analytical grade and used as received. RGM-PSF membranes were prepared by using the phase inversion method [34,35]. The prepared membrane was rinsed with deionized water and then washed by phosphate buffer solution (PBS, 0.05 M, pH 7.0) for three times before use.

3.2. Construction of EMBR

RGM-PSF membranes were sealed using polysiloxane glue to make a dead-end filtration membrane module. The effective length of each membrane was 10 cm and the membrane number was six. The prepared RGM-PSF membrane module was placed in a dead-end filtration apparatus to construct a membrane bioreactor (Figure S2). An appropriate amount of CRL powder was dissolved in PBS (0.05 M, pH 7.0) to prepare a $2.5 \text{ mg}\cdot\text{mL}^{-1}$ of CRL solution. Insoluble impurities of the enzyme solution were removed by centrifugation at $5000 \text{ r}\cdot\text{min}^{-1}$ for 10 min. Prior to enzyme immobilization, the bioreactor was thoroughly rinsed with de-ionized water, and then rinsed with PBS (0.05 M, pH 7.0) for 20 min. In the enzyme immobilization process, CRL solution was stirred continuously and filtrated from the inner surface of the membrane to the outer surface under a fluid velocity of $700 \mu\text{L}\cdot\text{min}^{-1}$. Afterward, the CRL immobilized membranes were washed with PBS (0.05 M, pH 7.0) at a higher fluid velocity of $800 \mu\text{L}\cdot\text{min}^{-1}$ to remove weakly adsorbed enzymes, until no protein was detected in the washings. The concentration of enzyme protein in the solution was determined by a method reported by Bradford with a calibration curve of BSA constructed for standard [36]. Enzyme loading was defined as the amount of enzyme (mg) adsorbed on per gram of RGM-PSF membrane, which was calculated from the protein mass balance among the enzyme solutions before and after immobilization and the washings. Each value was the mean of at least three parallel experiments, and the standard deviation was within approximately 5%.

The size of free CRL in PBS (0.05 M, pH 7.0) was measured by a particle size analyzer (NanoBrook 90 Plus, Brookhaven Instruments Corp., Holtsville, NY, USA). A field-emission scanning electron microscope (FE-SEM, S4800, Hitachi, Tokyo, Japan) was used to observe the cross-sectional morphologies of the RGM-PSF membrane before and after immobilization, with the accelerating

voltage of 3 kV and sample distance of 15 mm. Membrane pore size was measured with a liquid-liquid displacement porometer (LLP-1200A, Porous Materials Inc., Ithaca, NY, USA) according to the Yong–Laplace equation; and in this measurement, galwick and isopropanol were used as the fluid. An energy dispersive X-ray spectrometer (EDX, S4800, Hitachi, Tokyo, Japan) was utilized to map the distribution of nitrogen, which can present the distribution of CRL immobilized on the membrane. In this characterization, the accelerating voltage was 20 kV and the distance between the sample and the detector was 15 mm. A fluorescence microscope (Ti-U, Nikon, Tokyo, Japan) were used to detect the existence of FITC-CRL immobilized on the membrane, and in this test, the concentration of FITC-CRL solution was 20 µg/mL.

3.3. TA Hydrolysis in EMBR

The hydrolysis of TA was conducted in a similar dead-end filtration way to CRL immobilization. 100 mL of TA solution was circulated through the CRL immobilized membranes at a specific operation pressure fixed by the peristaltic pump. The substrate reservoir was put in a water bath at a set temperature to keep the reaction temperature constant, and magnetic stirring was provided in order to enhance the mass transfer of the substrate as well as the product. TA was hydrolyzed by the immobilized CRL into glycerol diacetate, glycerol monoacetate, and glycerine, accompanied by acetic acid. As the solution circulated, free acetic acid dispersed into the substrate solution and was neutralized by adding a 0.1 M NaOH solution with an automatic titrator (ZD-2, Inesa Scientific Instrument Co., Ltd., Shanghai, China) to keep the pH value constant throughout the reaction process. The volume of NaOH solution consumed was recorded periodically to evaluate the reaction rate. Bioreactor activity was defined as the release of 1 µmol acetic acid per hour per gram of the membrane (dry weight) under the assay conditions. Each data was the average of at least three parallel experiments. Blank experiments were performed without immobilized CRL at the same assay conditions to subtract the effect of TA self-hydrolysis.

3.4. Reusability of EMBR

After one batch of hydrolysis operation, the bioreactor was thoroughly rinsed with PBS (0.05 M, pH 7.0) to remove any residual substrate and product; then a fresh substrate solution was circulated under the same experimental condition for another batch. Altogether nine batches were operated, and the operation time for each batch was 200 min. The relative activities of the bioreactor were normalized to the first batch operation.

4. Conclusions

An EMBR was constructed by immobilizing CRL on the RGM-PSF membrane through pressure-driven filtration. EMBR performance was studied by using enzymatic hydrolysis of TA as the model reaction and the effects of membrane pore diameter and substrate feed direction on the EMBR activity were investigated in detail. Results showed that pore diameter influenced the bioreactor activity by affecting the mass transfer resistance of the fluid in the membrane and the contact of the substrate with immobilized lipase, and a higher bioreactor activity was obtained under a feed direction of I/O. Moreover, operational parameters of operation pressure, substrate concentration and temperature were optimized to achieve a bioreactor activity up to $1.07 \times 10^4 \text{ U}\cdot\text{g}^{-1}$. This research exhibits the potential application of microfiltration membranes with a specific pore structure in the bio-catalytic field. What remains for future efforts is improving the operational stability of the EMBR to enable repeated usage in practical applications.

Supplementary Materials: The following are available online at <http://www.mdpi.com/2073-4344/9/6/495/s1>, Table S1: SEM images of the pristine RGM-PSF membranes with different pore sizes. The scale bar for the outer surface, inner surface, and cross-section is 1 µm, 2 µm, and 30 µm, respectively. Table S2: SEM images of the RGM-PSF membranes with different pore sizes after CRL immobilization. The scale bar for the outer surface, inner surface, and cross-section is 1 µm, 2 µm, and 30 µm, respectively. Table S3: Bioreactor efficiency under

different conditions. Figure S1: Particle size distribution of CRL dissolved in PBS (0.05 M, pH 7.0) measured by dynamic light scattering, Figure S2: Diagram of the EMBR.

Author Contributions: Conceptualization, X.-J.H.; validation, P.-C.C., Z.M., X.-Y.Z., D.-J.C., and X.-J.H.; formal analysis, P.-C.C., Z.M., and X.-Y.Z.; investigation, P.-C.C., Z.M., and X.-Y.Z.; resources, X.-J.H.; writing—original draft preparation, P.-C.C.; writing—review and editing, D.-J.C. and X.-J.H.; supervision, X.-J.H.; project administration, X.-J.H.; funding acquisition, X.-J.H.

Funding: This research was funded by the National Natural Science Foundation of China (Grant No. 61801160 and 21604032), and the Fundamental Research Funds for the Central Universities of China (Grant No.2018QNA4057).

Conflicts of Interest: The authors declare no conflict of interest. The funders had no role in the design of the study; in the collection, analyses, or interpretation of data; in the writing of the manuscript, or in the decision to publish the results.

References

1. Sheldon, R.A.; van Pelt, S. Enzyme immobilisation in biocatalysis: Why, what and how. *Chem. Soc. Rev.* **2013**, *42*, 6223–6235. [[CrossRef](#)] [[PubMed](#)]
2. Dhake, K.P.; Karoyo, A.H.; Mohamed, M.H.; Wilson, L.D.; Bhanage, B.M. Enzymatic activity studies of pseudomonas cepacia lipase adsorbed onto copolymer supports containing beta-cyclodextrin. *J. Mol. Catal. B Enzym.* **2013**, *87*, 105–112. [[CrossRef](#)]
3. Ranieri, G.; Mazzei, R.; Wu, Z.T.; Li, K.; Giorno, L. Use of a ceramic membrane to improve the performance of two-separate-phase biocatalytic membrane reactor. *Molecules* **2016**, *21*, 345. [[CrossRef](#)]
4. Cardenas-Fernandez, M.; Hamley-Bennett, C.; Leak, D.J.; Lye, G.J. Continuous enzymatic hydrolysis of sugar beet pectin and L-arabinose recovery within an integrated biorefinery. *Bioresour. Technol.* **2018**, *269*, 195–202. [[CrossRef](#)] [[PubMed](#)]
5. Morthensen, S.T.; Meyer, A.S.; Jorgensen, H.; Pinelo, M. Significance of membrane bioreactor design on the biocatalytic performance of glucose oxidase and catalase: Free vs. immobilized enzyme systems. *Biochem. Eng. J.* **2017**, *117*, 41–47. [[CrossRef](#)]
6. Mazurenko, I.; Etienne, M.; Kohring, G.W.; Lopicque, F.; Walcarius, A. Enzymatic bioreactor for simultaneous electrosynthesis and energy production. *Electrochim. Acta* **2016**, *199*, 342–348. [[CrossRef](#)]
7. Straathof, A.J.J.; Panke, S.; Schmid, A. The production of fine chemicals by biotransformations. *Curr. Opin. Biotechnol.* **2002**, *13*, 548–556. [[CrossRef](#)]
8. Liu, C.J.; Saeki, D.; Matsuyama, H. A novel strategy to immobilize enzymes on microporous membranes via dicarboxylic acid halides. *RSC Adv.* **2017**, *7*, 48199–48207. [[CrossRef](#)]
9. Mazzei, R.; Piacentini, E.; Gebreyohannes, A.Y.; Giorno, L. Membrane bioreactors in food, pharmaceutical and biofuel applications: State of the art, progresses and perspectives. *Curr. Org. Chem.* **2017**, *21*, 1671–1701. [[CrossRef](#)]
10. Guo, Y.Z.; Zhu, X.Y.; Fang, F.; Hong, X.; Wu, H.M.; Chen, D.J.; Huang, X.J. Immobilization of enzymes on a phospholipid bionically modified polysulfone gradient-pore membrane for the enhanced performance of enzymatic membrane bioreactors. *Molecules* **2018**, *23*, 144. [[CrossRef](#)] [[PubMed](#)]
11. Li, N.; Liu, L.F.; Yang, F.L. Highly conductive graphene/PANi-phytic acid modified cathodic filter membrane and its antifouling property in EMBR in neutral conditions. *Desalination* **2014**, *338*, 10–16. [[CrossRef](#)]
12. Liao, Y.; Tian, M.; Goh, S.W.; Wang, R.; Fane, A.G. Effects of internal concentration polarization and membrane roughness on phenol removal in extractive membrane bioreactor. *J. Membr. Sci.* **2018**, *563*, 309–319. [[CrossRef](#)]
13. Ovcharova, A.; Vasilevsky, V.; Borisov, I.; Bazhenov, S.; Volkov, A.; Bilydukevich, A.; Volkov, V. Polysulfone porous hollow fiber membranes for ethylene-ethane separation in gas-liquid membrane contactor. *Sep. Purif. Technol.* **2017**, *183*, 162–172. [[CrossRef](#)]
14. Lim, S.; Park, M.J.; Phuntsho, S.; Tijing, L.D.; Nisola, G.M.; Shim, W.G.; Chung, W.J.; Shon, H.K. Dual-layered nanocomposite substrate membrane based on polysulfone/graphene oxide for mitigating internal concentration polarization in forward osmosis. *Polymer* **2017**, *110*, 36–48. [[CrossRef](#)]
15. Lee, A.; Elam, J.W.; Darling, S.B. Membrane materials for water purification: Design, development, and application. *Environ. Sci. Water Res.* **2016**, *2*, 17–42. [[CrossRef](#)]
16. Poppe, J.K.; Fernandez-Lafuente, R.; Rodrigues, R.C.; Ayub, M.A.Z. Enzymatic reactors for biodiesel synthesis: Present status and future prospects. *Biotechnol. Adv.* **2015**, *33*, 511–525. [[CrossRef](#)]

17. Jochems, P.; Satyawali, Y.; Diels, L.; Dejonghe, W. Enzyme immobilization on/in polymeric membranes: Status, challenges and perspectives in biocatalytic membrane reactors (BMRs). *Green Chem.* **2011**, *13*, 1609–1623. [[CrossRef](#)]
18. Bali, N.; Petsi, A.J.; Skouras, E.D.; Burganos, V.N. Three-dimensional reconstruction of bioactive membranes and pore-scale simulation of enzymatic reactions: The case of lactose hydrolysis. *J. Membr. Sci.* **2017**, *524*, 225–234. [[CrossRef](#)]
19. Girono, L.; Drioli, E. Biocatalytic membrane reactors: Applications and perspectives. *Trends Biotechnol.* **2000**, *18*, 339–349. [[CrossRef](#)]
20. Okobira, T.; Matsuo, A.; Matsumoto, H.; Tanaka, T.; Kai, K.; Minari, C.; Goto, M.; Kawakita, H.; Uezu, K. Enhancement of immobilized lipase activity by design of polymer brushes on a hollow fiber membrane. *J. Biosci. Bioeng.* **2015**, *120*, 257–262. [[CrossRef](#)] [[PubMed](#)]
21. Liese, A.; Hilterhaus, L. Evaluation of immobilized enzymes for industrial applications. *Chem. Soc. Rev.* **2013**, *42*, 6236–6249. [[CrossRef](#)]
22. Rodrigues, R.C.; Ortiz, C.; Berenguer-Murcia, A.; Torres, R.; Fernandez-Lafuente, R. Modifying enzyme activity and selectivity by immobilization. *Chem. Soc. Rev.* **2013**, *42*, 6290–6307. [[CrossRef](#)]
23. Nogalska, A.; Ammendola, M.; Portugal, C.A.M.; Tylkowski, B.; Crespo, J.G.; Garcia-Valls, R. Polysulfone biomimetic membrane for CO₂ capture. *Funct. Mater. Lett.* **2018**, *11*, 1850046. [[CrossRef](#)]
24. Mahlicli, F.Y.; Sen, Y.; Mutlu, M.; Altinkaya, S.A. Immobilization of superoxide dismutase/catalase onto polysulfone membranes to suppress hemodialysis-induced oxidative stress: A comparison of two immobilization methods. *J. Membr. Sci.* **2015**, *479*, 175–189. [[CrossRef](#)]
25. Gupta, S.; Ingole, P.; Singh, K.; Bhattacharya, A. Comparative study of the hydrolysis of different oils by lipase-immobilized membranes. *J. Appl. Polym. Sci.* **2012**, *124*, E17–E26. [[CrossRef](#)]
26. Saeki, D.; Nagao, S.; Sawada, I.; Ohmukai, Y.; Maruyama, T.; Matsuyama, H. Development of antibacterial polyamide reverse osmosis membrane modified with a covalently immobilized enzyme. *J. Membr. Sci.* **2013**, *428*, 403–409. [[CrossRef](#)]
27. Liu, J.G.; Cui, Z.F. Optimization of operating conditions for glucose oxidation in an enzymatic membrane bioreactor. *J. Membr. Sci.* **2007**, *302*, 180–187. [[CrossRef](#)]
28. Wang, Z.G.; Wang, J.Q.; Xu, Z.K. Immobilization of lipase from *Candida rugosa* on electrospun polysulfone nanofibrous membranes by adsorption. *J. Mol. Catal. B Enzym.* **2006**, *42*, 45–51. [[CrossRef](#)]
29. Sousa, H.A.; Rodrigues, C.; Klein, E.; Afonso, C.A.M.; Crespo, J.G. Immobilisation of pig liver esterase in hollow fibre membranes. *Enzym. Microb. Tech.* **2001**, *29*, 625–634. [[CrossRef](#)]
30. Andre, J.; Borneman, Z.; Wessling, M. Enzymatic conversion in ion-exchange matrix hollow fiber membranes. *Ind. Eng. Chem. Res.* **2013**, *52*, 8635–8644. [[CrossRef](#)]
31. Chen, P.C.; Huang, X.J.; Xu, Z.K. Utilization of a biphasic oil/aqueous cellulose nanofiber membrane bioreactor with immobilized lipase for continuous hydrolysis of olive oil. *Cellulose* **2014**, *21*, 407–416. [[CrossRef](#)]
32. Ulbricht, M.; Riedel, M.; Marx, U. Novel photochemical surface functionalization of polysulfone ultrafiltration membranes for covalent immobilization of biomolecules. *J. Membr. Sci.* **1996**, *120*, 239–259. [[CrossRef](#)]
33. Zhu, X.Y.; Chen, C.; Chen, P.C.; Gao, Q.L.; Fang, F.; Li, J.; Huang, X.J. High-performance enzymatic membrane bioreactor based on a radial gradient of pores in a PSF membrane via facile enzyme immobilization. *RSC Adv.* **2016**, *6*, 30804–30812. [[CrossRef](#)]
34. Huang, X.J.; Wang, L.W.; Zhang, L.L.; Gao, Q.L. Superhydrophilic and Gradient Hole Structured Hollow Fiber Membrane. CN201410081610.9, 28 May 2014.
35. Gao, Q.L.; Fang, F.; Chen, C.; Zhu, X.Y.; Li, J.; Tang, H.Y.; Zhang, Z.B.; Huang, X.J. Facile approach to silica-modified polysulfone microfiltration membranes for oil-in-water emulsion separation. *RSC Adv.* **2016**, *6*, 41323–41330. [[CrossRef](#)]
36. Bradford, M.M. A rapid and sensitive method for the quantitation of microgram quantities of protein utilizing the principle of protein-dye binding. *Anal. Biochem.* **1976**, *72*, 248–254. [[CrossRef](#)]

